ELSEVIER

Lithos 39 (1996) 1–20

LITHOS

Geochemistry of the Karamea Batholith, New Zealand and comparisons with the Lachlan Fold Belt granites of SE Australia

R.J. Muir [a,*], S.D. Weaver [a], J.D. Bradshaw [a], G.N. Eby [b], J.A. Evans [c], T.R. Ireland [d]

[a] *Department of Geological Sciences, University of Canterbury, Private Bag 4800, Christchurch, New Zealand*
[b] *Department of Earth Sciences, University of Massachusetts, Lowell, MA 01854, USA*
[c] *NERC Isotope Geosciences Laboratory, British Geological Survey, Keyworth, Nottingham NG12 5GG, UK*
[d] *Research School of Earth Sciences, The Australian National University, 1 Mills Road, Canberra, ACT 0200, Australia*

Received 4 January 1996; revised 7 June 1996; accepted 7 June 1996

Abstract

The Karamea Batholith in the Buller terrane of the South Island New Zealand forms part of an extensive Middle–Late Devonian belt of magmatic activity along, or close to, the Paleo-Pacific margin of Gondwana. The belt includes the I- and S-type granites of the Lachlan Fold Belt in SE Australia and coeval rocks in Antarctica. The northern half of the Karamea Batholith comprises five main intrusive phases: Zetland Diorite, Whale Creek Granite, Karamea Granite, O'Sullivans Granite and Dunphy Granite. To the east of the Karamea Batholith in the Takaka terrane, ultramafic–mafic Devonian igneous rocks are represented by the Riwaka Complex.

The rocks forming the Karamea Batholith are a high-K calc-alkaline suite ranging in composition from metaluminous (ASI for Zetland Diorite = 0.8) to strongly peraluminous (ASI for Dunphy Granite = 1.2–1.3). Initial $^{87}Sr/^{86}Sr$ ratios exhibit a large range from 0.705 in the Zetland Diorite to 0.719 in the Dunphy Granite. The corresponding values for ϵ_{Nd} are −0.3 and −9.2. There is a strong inverse correlation between ϵ_{Nd} and initial $^{87}Sr/^{86}Sr$, which suggests that the Karamea rocks were generated by a simple mixing process. The mafic end-member (with $\epsilon_{Nd} = 0$), which is itself probably derived from a mixed lithospheric source, is taken to be the Zetland Diorite/Riwaka Complex, and the crustal end-member is represented by Ordovician Greenland Group greywackes that form the country rocks to the batholith. Mixing is also supported by recent U–Pb zircon studies. The inherited zircon population in the granites matches the detrital zircon population in the Greenland Group greywackes. The Whale Creek Granite, Karamea Granite and O'Sullivans Granite can be modelled by 20–30% crustal material, whereas the Dunphy Granite appears to represent 65–85% crustal material.

In terms of the I–S classification scheme developed for the Lachlan Fold Belt granites in SE Australia, both types are present in the Karamea Batholith. However, in New Zealand there appears to be a continuum from one extreme to the other, which is consistent with the mixing model presented here.

Keywords: igneous; geochemistry; granite; New Zealand; Devonian; Gondwana

* Corresponding author. Present address: Isotope Geosciences Unit, Scottish Universities Research and Reactor Centre, East Kilbride, Glasgow, G75 OQU and Department of Geology and Applied Geology, University of Glasgow, Glasgow G12 8QQ, Scotland, UK. E-mail: muir@geology.gla.ac.uk.

PII S0024-4937(96)00017-5

1. Introduction

The I- and S-type classification of granites proposed by Chappell and White (1974) for the Lachlan Fold Belt in SE Australia has been a widely used concept in igneous petrology for the past twenty years. I-type stands for *infracrustal* or *igneous* protolith, and S-type for *supracrustal* or *sedimentary* protolith. Both types of granite are regarded as essentially crustal melts and are distinguished on the basis of a set of mineralogical, chemical and isotopic criteria (see Chappell and White (1992) for a recent review). Chemical variation within the granite suites in SE Australia has been attributed largely to different degrees of unmixing of SiO_2-poor restite and SiO_2-rich melt fractions (White and Chappell, 1977). However, Phillips et al. (1981), Wall et al. (1987) and Collins (in press) have argued that the within suite chemical variation can be explained equally well by crystal fractionation. Gray (1984, 1990, 1995) proposed that granite genesis involved mixing of basaltic material and granitic melt derived from metasedimentary rocks, rather than restite unmixing. More recently, Collins (in press) has suggested that the I- and S-type granites are products of a three component mixing system.

Time equivalents of the Caledonian age (440–380 Ma) granites in the Lachlan Fold Belt also occur in New Zealand and Antarctica (e.g. Muir et al., 1994, 1996, and references therein). These plutonic rocks are presently scattered around the borderlands of the Southern Ocean, but were almost certainly contiguous prior to the break-up of Gondwana during the late Mesozoic. In this paper we present the first detailed account of the geochemistry of the Middle–Late Devonian Karamea Batholith in the South Island of New Zealand. Our preferred petrogenetic model for the Karamea granites is discussed in terms of those developed for the Lachlan Fold Belt granites.

2. Geological setting

The Western Province of New Zealand (Landis and Coombs, 1967) is confined to the NW and SW parts of the South Island. It extends offshore, probably at least to the Campbell Plateau in the SE and the Lord Howe Rise in the NW (Fig. 1a), and represents a fragment of Gondwana that separated from SE Australia and Antarctica as a result of late Mesozoic crustal extension and seafloor spreading (e.g. Mayes et al., 1990; Weaver et al., 1994).

In the NW Nelson–Westland region (Fig. 1a), Cooper (1989) has divided the Western Province into two Paleozoic terranes separated by the north–south trending Anatoki Thrust. In the west, the Buller terrane consists largely of Ordovician quartz-rich turbiditic sandstones (mainly Greenland Group greywackes) and graptolitic shales. The Takaka terrane to the east is lithologically much more diverse, and includes Cambrian volcanic and volcaniclastic rocks, Ordovician carbonate sequences and Silurian quartzites. Both terranes have small outliers of Lower Devonian rocks, although these differ in character.

Granitic rocks and related diorites make up approximately 50% of the total area of the Western Province. Those in NW Nelson–Westland have been reviewed briefly by Tulloch (1983, 1988), who has identified the major batholiths and compositional suites (Fig. 1a). Middle–Late Devonian age granites appear to be restricted to the Buller terrane and make up the bulk of the Karamea Batholith, the largest contiguous tract of igneous rocks in the Western Province. Individual zircon crystals from the main intrusive phases forming the batholith have recently been dated by ion-microprobe (SHRIMP) mass-spectrometry at 375 ± 5 Ma (Muir et al., 1994, 1996). In the Takaka terrane, ultramafic–mafic igneous rocks with similar ages are represented by the Riwaka Complex (Gill and Johnston, 1970). Harrison and McDougall (1980) obtained K–Ar ages of ~ 370 Ma on hornblende crystals from the Rameka Gabbro at the northern end of the complex. Further south, a sample of the Brooklyn Diorite yielded a U–Pb zircon age of 376.9 ± 5.6 Ma (2σ), indicating emplacement coeval with the Karamea Batholith (Muir et al., 1996). Paleozoic granites are also known in Fiordland and on Stewart Island (southern South Island), and almost certainly represent a continuation of the Karamea Batholith disrupted by Cenozoic movement on the Alpine Fault system.

3. Karamea Batholith — field relationships and petrography

The Karamea Batholith extends south from Kahurangi Point for nearly 200 km to the Alpine Fault

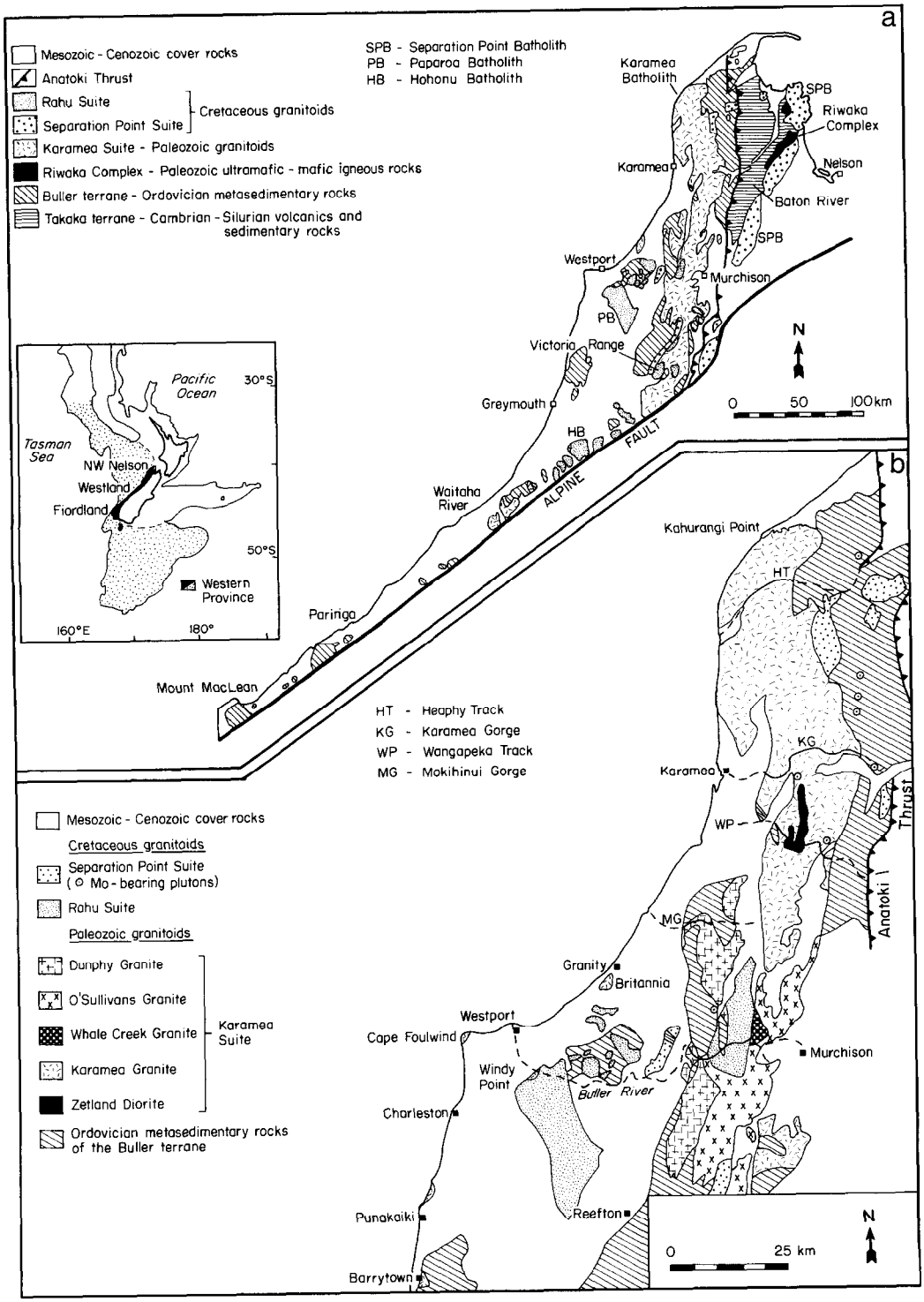

Fig. 1. (a) Geological map of NW Nelson–Westland showing the distribution of granitoid rocks and the location of the Karamea Batholith (after Muir et al., 1994). (b) Geological map of the northern part of the Karamea Batholith (after Muir et al., 1996).

east of Greymouth, and has an average width of 20 km (Fig. 1a). It intrudes Ordovician metasedimentary rocks of the Greenland Group to the west and the Golden Bay Group to the east (Cooper, 1989). Large, stoped blocks of country rock are common near the steeply dipping margins of the batholith, and biotite, andalusite, sillimanite and cordierite have been observed in the contact aureole, which is generally < 1 km wide (Roder and Suggate, 1990). The batholith is associated with weak Sn–W mineralisation (Braithwaite and Pirajno, 1993) and is cut by several Cretaceous (Separation Point Suite and Rahu Suite) plutons, but these are not volumetrically significant. Devonian granites compositionally equivalent to those of the main batholith also occur to the west and southwest of the main batholith (e.g. at Granity, Meybille Bay, Barrytown, the Waitaha River, Paringa, Mount MacLean and within the Hohonu Batholith) and small Carboniferous plutons (~ 330 Ma) occur on the coast at Cape Foulwind and at Windy Point in the Lower Buller Gorge (Fig. 1).

Most of the Karamea Batholith is relatively inaccessible and poorly exposed below the bushline, and thus has been little studied. Following a recent field mapping and geochemical sampling programme, covering the batholith north of the Victoria Range, we have identified five major intrusive phases (Fig. 1b). Their distribution and petrography are outlined below. More detailed petrographic descriptions, including modal data, can be found in Nathan (1978) and Roder and Suggate (1990).

3.1. Karamea granite

The dominant lithology, forming the northern two-thirds of the batholith and a smaller body south of Murchison (Fig. 1b), is a coarse-grained, porphyritic biotite granite (syenogranite–monzogranite), termed the Karamea Granite after Grindley (1961). It is a distinctive unit, containing large, pink, prismatic alkali-feldspar megacrysts (30–40 mm in length) in a groundmass of quartz, oligoclase, microcline, biotite, and muscovite with accessory apatite, zircon and iron oxide. The alkali feldspar megacrysts — orthoclase, microcline, or microperthite — are generally kaolinised and bright pink in colour, although white alkali feldspar or plagioclase phenocrysts are also common locally (e.g., Karamea Gorge and Wangapeka Track areas). The megacrysts often show a strong preferred orientation, probably as a result of magmatic flow. The Karamea Granite exhibits comagmatic (mingling) field relationships with dioritic rocks in the Wangapeka Track area, but its position in the overall order of emplacement is not known. The Brittania Granite pluton, south of Granity (Fig. 1b), has been correlated with the Karamea Granite by Nathan (1978) and Kutsukake (1988).

3.2. Whale Creek Granite

The Whale Creek Granite (Roder and Suggate, 1990) forms a small pluton (~ 20 km^2) at the eastern end of the Upper Buller Gorge (Fig. 1b). It is a coarse-grained, dark grey, porphyritic biotite-granite, with large, white, tabular alkali feldspar megacrysts (typically 30–40 mm in length). In places, a well developed foliation is defined by aligned megacrysts and flakes of dark brown to reddish-brown biotite. A few flakes of muscovite have also been found. Roder and Suggate (1990) have correlated the Whale Creek Granite with the Karamea Granite further north on the basis of petrographic similarities. However, the Whale Creek Granite is considerably more mafic and can also be distinguished from the Karamea Granite on geochemical grounds, having a lower SiO_2 and higher total Fe_2O_3 content. The Whale Creek Granite is cut by sheets of O'Sullivans Granite in the Upper Buller Gorge.

3.3. O'Sullivans Granite

The O'Sullivans Granite (Roder and Suggate, 1990) is the dominant phase along the eastern side of the batholith in the vicinity of the Upper Buller Gorge (Fig. 1b), extending south to the Victoria Range and north to the Matiri Range. It is a fine to medium grained, pale grey, muscovite–biotite granite with sparse phenocrysts of plagioclase or alkali feldspar up to 15 mm in length. Irregular sheets and patches of finer-grained aplitic material within the granite have been termed the Fern Flat Granite Aplite by Roder and Suggate (1990).

3.4. Dunphy Granite

The Dunphy Granite (Nathan, 1978) occurs in the western part of the Upper Buller Gorge (Fig. 1b),

extending south along the Brunner Range, and north to the Glasgow Range and the Mohikinui Gorge. It is a coarse-grained leucocratic muscovite–biotite granite with abundant phenocrysts of white alkali feldspar (typically 25 × 10 mm). The phenocrysts are commonly aligned, probably as a result of magmatic flow. Cordierite has been found in two samples from the Buller Gorge area and occurs as small (< 0.5 mm) subhedral crystals showing complex twinning. The Dunphy Granite has not been observed in contact with any other intrusive phases.

3.5. Zetland Diorite

Fine to coarse-grained biotite and biotite–hornblende quartz diorites crop out extensively around Mount Zetland and along the Herbert Range north of the Wangapeka Track (Fig. 1b). These mafic rocks have an areal extent of ~ 25 km^2 and irregular contact relationships with the enclosing Karamea Granite suggest that mingling of felsic and mafic magmas occurred. The dominant rock type contains green-brown biotite (~ 25%), hornblende (after pyroxene) (~ 25%) and plagioclase (andesine) (~ 40%), with lesser amounts of quartz, alkali feldspar, apatite, iron oxides and titanite. Igneous textures are dominant, but recrystallisation to amphibolite is common.

3.6. Enclaves

Metasedimentary enclaves of the Greenland Group greywacke are rare in the Karamea Granite, but are common in the O'Sullivans Granite and Dunphy Granite. They range in size from a few centimetres to several tens of metres, and many show signs of partial assimilation. No enclaves have been found in the Whale Creek Granite or Zetland Diorite.

4. Riwaka complex — field relationships and petrography

The Riwaka Complex (Gill and Johnston, 1970), which lies to the east of the Karamea Batholith (Fig. 1a), intrudes Lower Paleozoic metasedimentary rocks in the west Nelson area. The complex occupies an area of ~ 100 km^2 and consists of elongate sheets of ultramafic–gabbroic rocks and pyroxene-bearing diorite–monzodiorite. Grindley (1980), suggested that the complex, which is associated with Ni and Cu mineralisation, was intruded as a layered lopolith along the axis of a major synclinal structure. The northern part of the intrusion was referred to by Grindley (1971) as the Rameka Diorite (a gabbro). The southern part of the intrusion is a narrow (1 km) concordant sheet of olivine pyroxenite and peridotite that has been interpreted as a feeder dike. The rocks become more felsic and the complex widens to the northeast. The most felsic rock, known as the Brooklyn Diorite (Grindley, 1980), represents the upper part of the layered intrusion. The rock contains clinopyroxene with exsolved brown hornblende, plagioclase (andesine), and interstitial biotite, orthopyroxene, quartz, alkali feldspar, apatite, iron oxides and titanite. Igneous textures are dominant, but recrystallisation to amphibolite is common.

5. Geochemistry

Tulloch (1983, 1988) and Cooper and Tulloch (1992) have classified the bulk of the Paleozoic granitoids in the Western Province as S-type on the basis of limited petrographic and geochemical data. However, it will be seen from the following sections that the Karamea Batholith comprises both I- and S-type granites (sensu Chappell and White, 1974).

5.1. Major and trace elements

Representative data from a set of 95 analysed rocks from the Karamea Batholith are given in Table 1. For comparative purposes, a sample of the Rameka Gabbro and a sample of the Brooklyn Diorite from the Riwaka Complex were also analysed. All samples were carefully selected to avoid the effects of secondary alteration. On an AFM diagram the Karamea samples define a typical calc-alkaline trend and have a Peacock index of c. 60 (Fig. 2), confirming a calc-alkalic designation. SiO_2 contents for the granitoid samples are in a relatively narrow range from 62–77 wt.%. There is a distinct compositional gap between the Zetland Diorite (SiO_2 ~ 50 wt.%) and the granite samples. On a plot of K_2O vs. SiO_2 (Fig. 3), most of the samples fall into the field

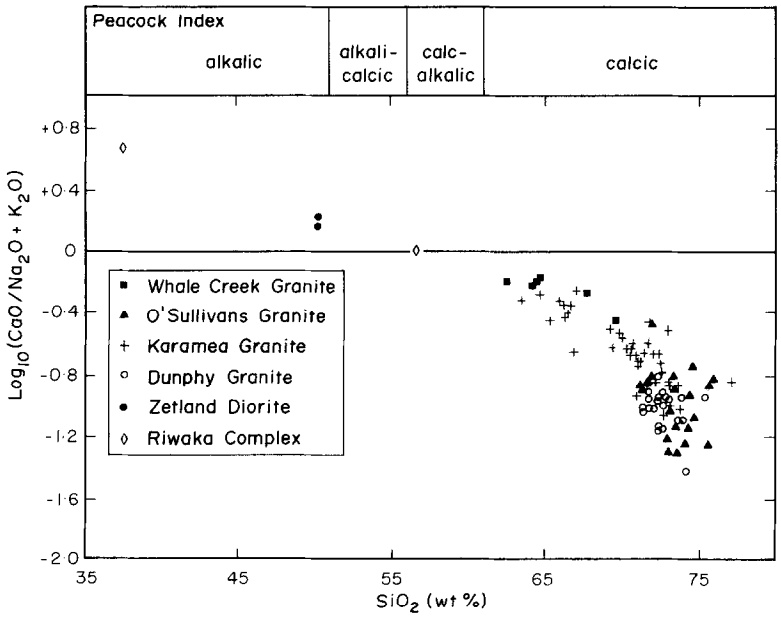

Fig. 2. Peacock Index diagram (after Brown, 1982). The Peacock Index for a particular rock suite is calculated from the point where the data trend crosses the $\log_{10}(CaO/K_20 + Na_2O)$ value.

defined as high-K calc-alkaline by Ewart (1982). On a plot of K_2O vs. Na_2O (Fig. 4), nearly all of the samples fall within the field of I-type granites from the Lachlan Fold Belt (White and Chappell, 1983).

Classification by the alumina saturation index (ASI) of Zen (1986) indicates that all of the granite samples are peraluminous (ASI > 1) (Fig. 5). The two samples of Zetland Diorite are strongly metaluminous (ASI = 0.86) and the Whale Creek Granite is weakly peraluminous (ASI = 1.0–1.1). The Karamea Granite and O'Sullivans Granite are moderately peraluminous (ASI = 1.0–1.2) and the Dunphy Granite is strongly peraluminous (ASI = 1.2–1.3).

Major and trace element variations are illustrated on selected Harker diagrams in Fig. 3, and show typical fractional crystallisation trends. TiO_2, Al_2O_3, $Fe_2O_3^*$, MnO, MgO, CaO and P_2O_5 all show a negative correlation with SiO_2. Na_2O exhibits a wide range of values for samples of similar SiO_2 content, with generally higher values (> 2wt.%) in the Zetland Diorite, Karamea Granite and O'Sullivans Granite, and lower values (< 2wt.%) in the Whale Creek Granite and Dunphy Granite. In contrast, K_2O increases steadily with increasing SiO_2. The trace elements tend to exhibit more scatter than the major elements, but V, Cr, Ni, Zn, Zr, Y, Ba and Sr generally decrease and Rb increases with increasing SiO_2.

Rare earth element data (REE) for the batholith are plotted on a chondrite normalized diagram in Fig. 6. All of the samples have moderate negative Eu anomalies suggesting feldspar fractionation. Eu/Eu^* decreases from 0.8 in the Zetland Diorite to 0.7 in the Whale Creek Granite, 0.5 in the Dunphy Granite and 0.3 in the Karamea Granite and O'Sullivans Granite. Total REE contents decrease with increasing SiO_2 (wt.%) and ASI. In addition, there is a systematic increase in the fractionation of the REE, with Ce_N/Yb_N ratios ranging from ~ 3 in the Zetland Diorite to ~ 20 in the Dunphy Granite. The REE variations are probably governed by crystallisation of accessory phases such as apatite, monazite and zircon, which are the main carriers of the REE in such peraluminous granitic rocks (e.g. Mittlefehldt and Miller, 1983).

On a multi-element variation diagram (Fig. 7), the granites are characterized by marked negative Ti, P, Sr, Nb and Ba anomalies, relatively high levels of Rb, Th and U, and low K/Rb. The negative anomalies indicate fractionation by mineral phases contain-

ing these elements at some stage in the history of the source or of the magma. The negative Nb anomaly, which is often taken to characterise subduction-related magmas (e.g. McCulloch and Gamble, 1991), is also present in the Zetland Diorite (Fig. 7) and is therefore probably inherited from the source region. The spidergram patterns for the Karamea granites are closely similar to the patterns for average I- and S-type granite from the Lachlan Fold Belt (Fig. 7).

The limited amount of data available from the Riwaka Complex precludes a rigorous comparison with Karamea Batholith. It is apparent from Table 1, nevertheless, that the whole-rock compositions of the Zetland Diorite bear a close resemblance to the Brooklyn Diorite from the Riwaka Complex. Both have a typical "continental" trace element signature (Fig. 7): showing enrichment in the large ion lithophile (LIL) and light REE and depletion in the

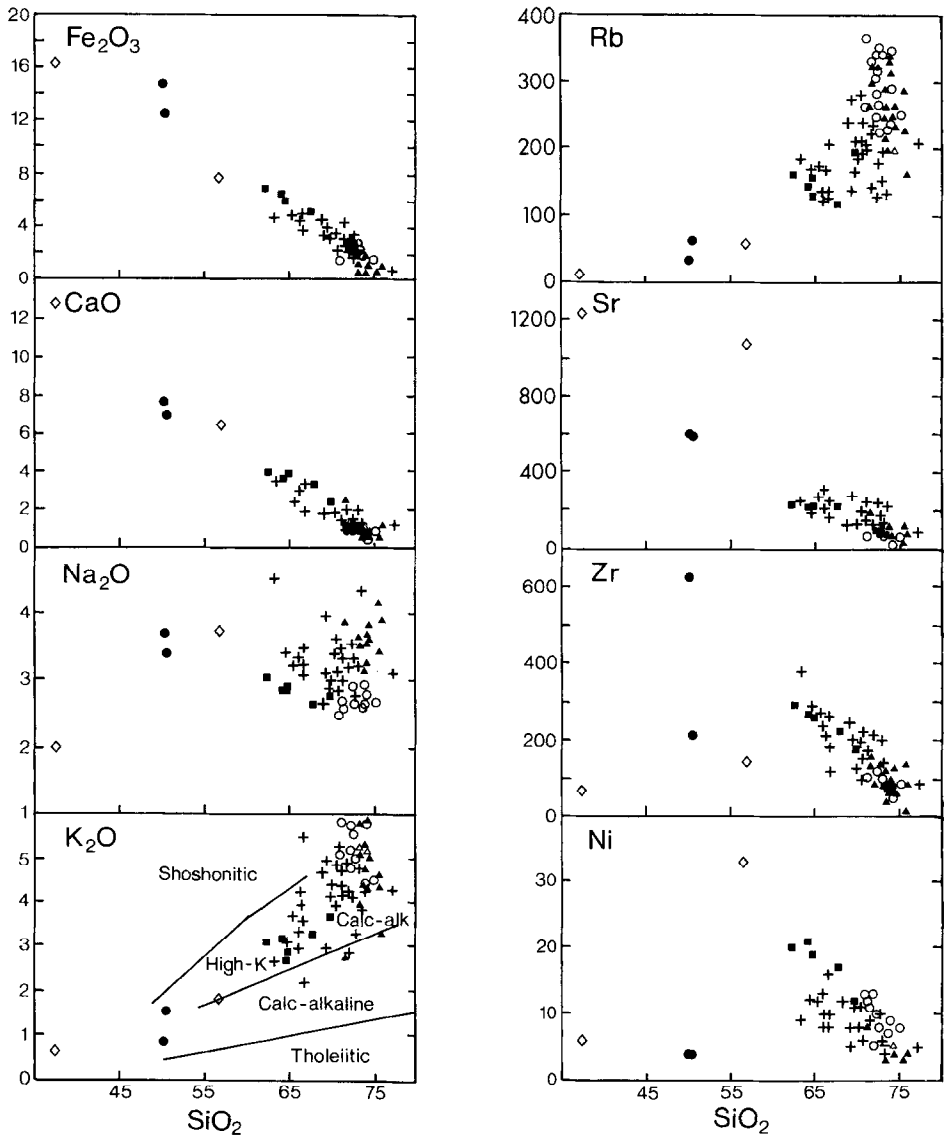

Fig. 3. Selected Harker plots to illustrate the variations of major and trace elements in the Karamea Batholith. The K_2O vs. SiO_2 diagram shows the High-K calc-alkaline nature of the batholith. Field boundaries from Ewart (1982).

Table 1
Representative analyses of the Karamea Batholith

	Whale Creek Granite		O'Sullivans Granite		Dunphy Granite				Karamea Granite			Barrytown Granite	Zetland Diorite		Riwaka Complex	
	RNZ 169	RNZ 173	RNZ 120	RNZ 271	RNZ 194	RNZ 199	RNZ 212	RNZ 222	RNZ 230	RNZ 252	RNZ 261	BA	RNZ 253	RNZ 254	RNZ 25	RNZ275
Major elements (wt.% oxides)																
SiO_2	64.64	64.73	72.73	75.67	72.54	75.05	71.05	71.80	71.59	72.38	70.88	68.92	50.14	50.47	37.35	56.69
TiO_2	0.99	1.01	0.31	0.08	0.25	0.20	0.23	0.43	0.46	0.30	0.44	0.71	1.63	1.91	2.61	1.29
Al_2O_3	15.42	15.35	14.54	13.37	14.56	13.36	14.94	14.58	14.31	14.56	14.37	14.48	17.99	17.17	18.20	15.98
Fe_2O_3	6.12	6.00	2.03	1.35	1.64	1.51	1.43	2.65	3.03	2.20	2.79	4.55	14.73	12.46	16.23	7.68
MnO	0.07	0.07	0.02	0.02	0.02	0.02	0.02	0.03	0.06	0.03	0.04	0.06	0.26	0.23	0.17	0.14
MgO	2.10	2.05	0.52	0.16	0.62	0.49	0.47	1.07	0.88	0.85	0.80	1.26	2.28	3.38	6.30	3.90
CaO	3.71	3.84	0.96	1.07	0.95	0.85	0.70	1.17	1.91	1.42	1.48	1.77	7.65	6.95	12.77	6.39
Na_2O	2.85	2.90	2.88	3.42	2.82	2.67	2.84	2.62	3.28	3.31	2.92	2.65	3.70	3.40	1.99	3.73
K_2O	2.69	2.86	5.31	4.32	5.34	4.50	5.84	5.15	4.11	4.21	5.24	4.65	0.86	1.51	0.61	1.79
P_2O_5	0.31	0.31	0.25	0.06	0.23	0.21	0.27	0.22	0.18	0.13	0.20	0.25	0.64	0.89	1.68	0.48
LOI	0.90	0.68	0.80	0.97	0.86	0.89	1.09	0.50	0.60	0.71	1.16	0.93	0.45	1.49	0.45	1.89
TOT	99.80	99.80	100.35	100.49	99.83	99.75	98.88	100.22	100.41	100.10	100.29	100.23	100.33	99.86	98.37	99.95
ASI	1.07	1.03	1.19	1.09	1.20	1.24	1.22	1.21	1.07	1.16	1.09	1.15	0.86	0.83	0.64	0.81

Trace elements (ppm)																
Ga	19	21	25	18	20	28	27	22	22	20	21	19	20	23	20	18
Pb	24	22	28	24	46	45	44	38	34	36	43	30	6	14	5	10
Rb	157	130	232	227	266	251	268	259	221	222	281	241	34	61	7	53
Sr	222	225	84	120	83	62	64	103	113	116	116	118	602	583	1231	1079
Y	32	32	21	17	13	11	16	22	45	22	29	40	75	52	35	20
V	89	94	16	9	18	20	15	33	34	31	34	36	8	96	280	143
Cr	40	39	13	3	14	10	8	24	13	12	12	22	6	6	10	74
Ni	19	19	7	3	8	8	7	13	9	7	8	12	4	4	6	33
Zn	86	83	67	53	55	53	61	65	58	43	51	75	181	149	138	82
Zr	261	254	140	138	82	85	101	149	152	102	137	243	624	211	70	146
Nb	15	15	13	16	14	16	16	16	14	12	14	20	28	23	7	16
Ba	700	695	356	1131	273	178	241	426	246	300	388	496	291	354	184	522
Sc	13.8	14.7	3.6	6.0	2.8	2.7	2.3	5.4	6.8	4.6	5.9	9.6	46.3	36.3	29.4	16.1
Co	42.7	44.6	37.0	42.6	46.5	52.4	54.3	50.5	57.3	47.4	49.4	56.3	30.3	34.8	54.0	39.3
Cs	26.8	7.2	10.9	7.8	25.9	25.8	34.7	13.9	17.9	9.3	12.0	23.0	2.1	5.6	0.4	2.7
La	57.4	51.7	33.0	51.8	24.2	19.4	23.9	42.2	43.0	27.3	40.2	57.3	32.0	41.6	27.6	43.6
Ce	119.5	104.4	74.0	103.2	49.4	39.8	51.1	83.3	91.1	56.5	87.1	123.0	94.1	103.4	70.3	92.2
Nd	62.5	55.0	39.0	44.0	22.7	21.5	27.2	42.8	45.9	28.7	47.2	53.5	74.8	65.1	44.0	46.3
Sm	11.37	10.10	7.50	7.86	5.77	4.28	5.53	8.78	9.72	5.63	8.53	11.29	18.08	14.61	11.87	8.24
Eu	2.16	2.13	0.63	1.62	0.82	0.61	0.66	1.01	1.06	0.76	0.99	1.69	4.56	3.85	3.65	2.50
Gd	9.4	8.6	5.1	5.7	4.1	3.4	4.2	6.4	9.1	4.4	6.7	9.7	18.4	15.0	10.9	7.7
Tb	1.35	1.27	0.72	0.70	0.51	0.48	0.47	0.96	1.50	0.70	0.99	1.32	2.87	2.18	1.53	0.97
Ta	0.36	0.37	0.16	0.22	0.13	0.10	0.09	0.20	0.66	0.27	0.32	0.59	1.26	0.91	0.43	0.42
Yb	2.19	2.43	0.93	1.52	0.79	0.59	0.53	1.36	4.30	1.79	2.02	3.89	8.48	6.26	2.65	2.61
Lu	0.29	0.34	0.13	0.22	0.12	0.08	0.07	0.20	0.55	0.25	0.27	0.54	1.16	0.86	0.35	0.34
Hf	7.8	7.5	4.9	5.8	3.2	2.5	3.1	5.1	5.0	3.6	5.1	8.2	15.7	7.1	2.2	5.2
Ta	1.10	1.01	1.66	1.75	1.77	2.09	2.31	1.68	1.81	1.31	1.93	2.45	1.77	1.71	0.45	1.28
Th	19.5	17.3	23.3	17.1	11.9	8.8	13.1	20.6	25.3	16.4	27.2	28.2	2.2	4.9	1.6	7.1
U	1.74	1.84	4.28	3.85	7.82	8.61	4.41	4.11	5.91	3.93	4.57	3.64	1.26	1.44	0.67	2.02
Sb	0.20	3.52	0.50	1.63	3.48	0.23	0.36	0.79	2.76	0.00	0.00	2.19	3.60	0.53	2.63	2.61

Major and selected trace elements (Ga–Ba) by XRF analysis at University of Canterbury [Loss on ignition (LOI) at 1000°C, Fe as total Fe_2O_3], Sc–Sb values by INAA at University of Massachussets, Lowell. RNZ 25 = Rameka Gabbro, RNZ 275 = Brooklyn Diorite. Grid references for samples are given Table 2.

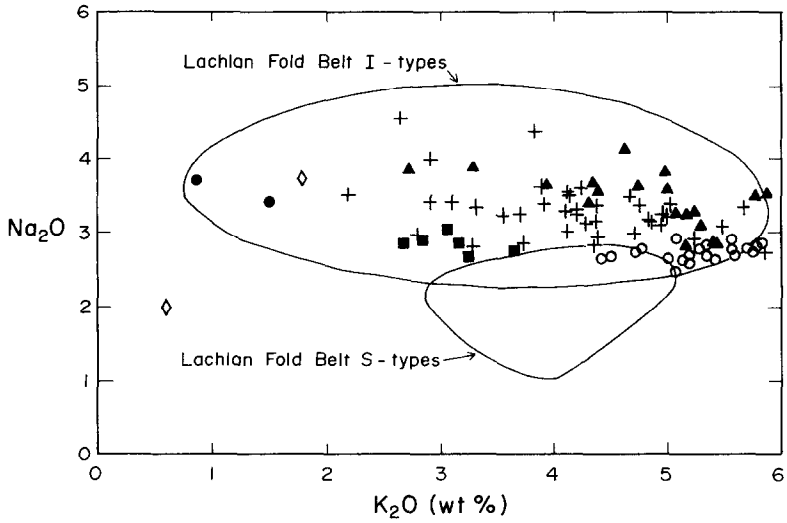

Fig. 4. Plot of Na_2O vs. K_2O for the Karamea Batholith. Fields for I- and S-type granites from the Lachlan Fold Belt after White and Chappell (1983).

high field strength (HFS) elements. In detail, the Brooklyn Diorite does not show a negative Sr anomaly and concentrations of the LIL elements are slightly higher and the HFS elements are slightly lower than in the Zetland Diorite. However, their multi-element patterns are closely similar and both are characterized by a negative Nb anomaly. The chondrite normalized REE pattern for the Zetland

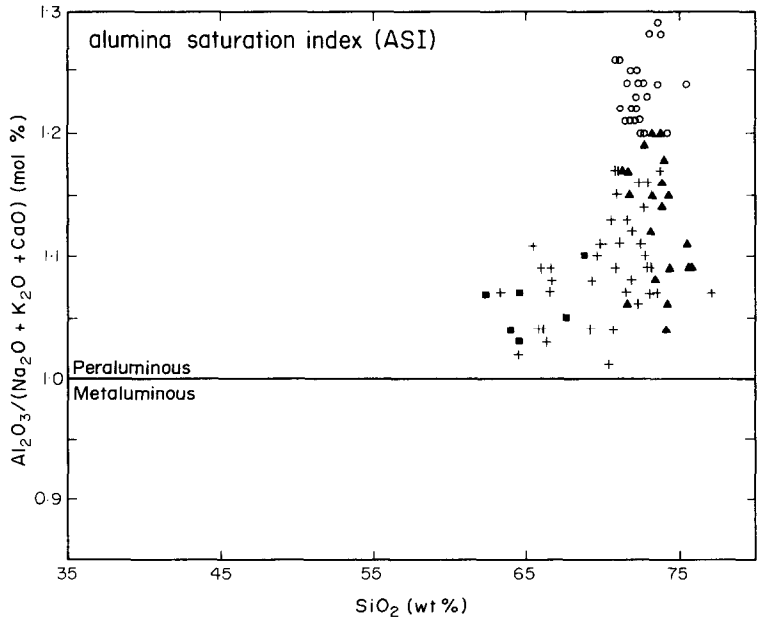

Fig. 5. Plot of mol. $Al_2O_3/(CaO + K_2O + K_2O)$ vs. SiO_2.

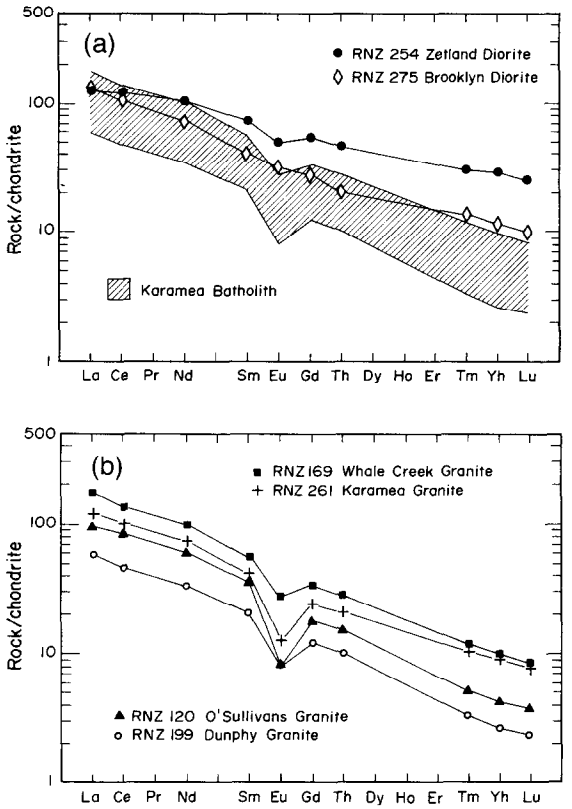

Fig. 6. REE abundance patterns for the Karamea Batholith, normalized to the chondrite data of Nakamura (1974).

Diorite shows a small negative Eu anomaly (Fig. 6), but the general slope of the pattern is clearly similar to the Brooklyn Diorite.

5.2. Sr and Nd isotopes

Samples for Sm–Nd analysis were spiked with ^{150}Nd and ^{147}Sm isotopically enriched tracers and decomposed using HF in teflon bombs at a temperature of 120°C for at least 48 h. This was followed by HNO_3 treatment and conversion to the chloride form using 6M HCl. Sr and the REE were separated by standard ion exchange procedures using Dowex AG50W-X12 ion exchange resin. Nd and Sm were further separated using cation resin columns and the di-2-ethylhexyl orthophosphoric acid coated teflon powder method (Richard et al., 1976).

Nd and Sm were loaded on Ta side filaments of a triple filaments assembly with Rh centre and analysed as metals. Measurements were made on a VG Micromass 354 fully automated, multiple collector, mass spectrometer. Three analyses of the La Jolla Nd isotope reference standard made during the period of this study yielded a $^{143}Nd/^{144}Nd$ ratio of 0.511862 $\pm$ 22 (2σ). Sr was loaded on single Ta filaments prepared with phosphoric acid. Measurements were made on a Finnigan Mat 262 instrument. The aver-

Table 2
Rb–Sr whole-rock data for the Karamea Batholith and related rocks

	Sample	Grid reference	Rb (ppm)	Sr (ppm)	$^{87}Rb/^{86}Sr$	$^{87}Sr/^{86}Sr$	$^{87}Sr/^{86}Sr$ (375 Ma)
Whale Creek Granite	RNZ 169	L29/438 360	157	222	2.05	0.719891 ± 7	0.70880
	RNZ 173	L29/431 357	130	225	1.67	0.718165 ± 7	0.70913
O'Sullivans Granite	RNZ 120	L29/438 359	313	83	11.00	0.767170 ± 7	0.70765
	RNZ 271	M29/527 468	227	120	5.49	0.735306 ± 7	0.70560
Dunphy Granite	RNZ 194	L29/315 322	266	83	9.33	0.768599 ± 7	0.71812
	RNZ 199	L29/286 326	251	62	11.70	0.782611 ± 8	0.71931
	RNZ 212	L28/311 544	368	64	16.80	0.805082 ± 8	0.71418
	RNZ 222	L23/294 609	259	103	7.31	0.753665 ± 7	0.71411
Karamea Granite	RNZ 230	L27/473 940	221	113	5.68	0.738176 ± 7	0.70744
	RNZ 252	M28/507 790	222	118	5.46	0.737016 ± 7	0.70747
	RNZ 261	L26/346 124	281	116	7.03	0.745903 ± 7	0.70787
Barrytown Granite	RNZ BA	K31/727 834	241	118	5.93	0.743499 ± 10	0.71141
Zetland Diorite	RNZ 254	M28/506 790	61	583	0.303	0.706482 ± 7	0.70484
Riwaka Complex	RNZ 275	N26/023 120	53	1079	0.142	0.705152 ± 7	0.70438

Grid references refer to the NZ 1:50,000 scale Topomap series.

age $^{87}Sr/^{86}Sr$ ratio determined for NBS 987 Sr isotope standard (10 analyses) was 0.710186 ± 16 (2σ).

Pickett and Wasserburg (1989) have previously used Sr and Nd isotopic data to demonstrate the involvement of older crustal material, similar to the Ordovician Greenland Group, in New Zealand granites. However, their data set contained only three samples of Paleozoic granite.

New Rb–Sr and Sm–Nd isotope data from the Karamea Batholith and related rocks are given in Tables 2 and 3, respectively. The samples exhibit a large range of $^{87}Rb/^{86}Sr$ ratios (0.163–16.8), but do not define a statistically acceptable isochron age because of the large variation in $^{87}Sr/^{86}Sr$ initial ratios (Table 2). $^{147}Sm/^{144}Nd$ ratios are similar to average continental crust (0.125), corresponding to light REE-enriched patterns (DePaolo and Wasserburg, 1976). Initial $^{87}Sr/^{86}Sr$ ratios and ϵ_{Nd} values have been calculated using a crystallisation age of 375 Ma (Muir et al., 1996) and are plotted in Fig. 8, together with the fields for contemporaneous rocks from Australia and Antarctica. There is a considerable spread in the initial $^{87}Sr/^{86}Sr$ ratios, with the Zetland Diorite showing the most primitive values (~ 0.705) and the strongly peraluminous Dunphy

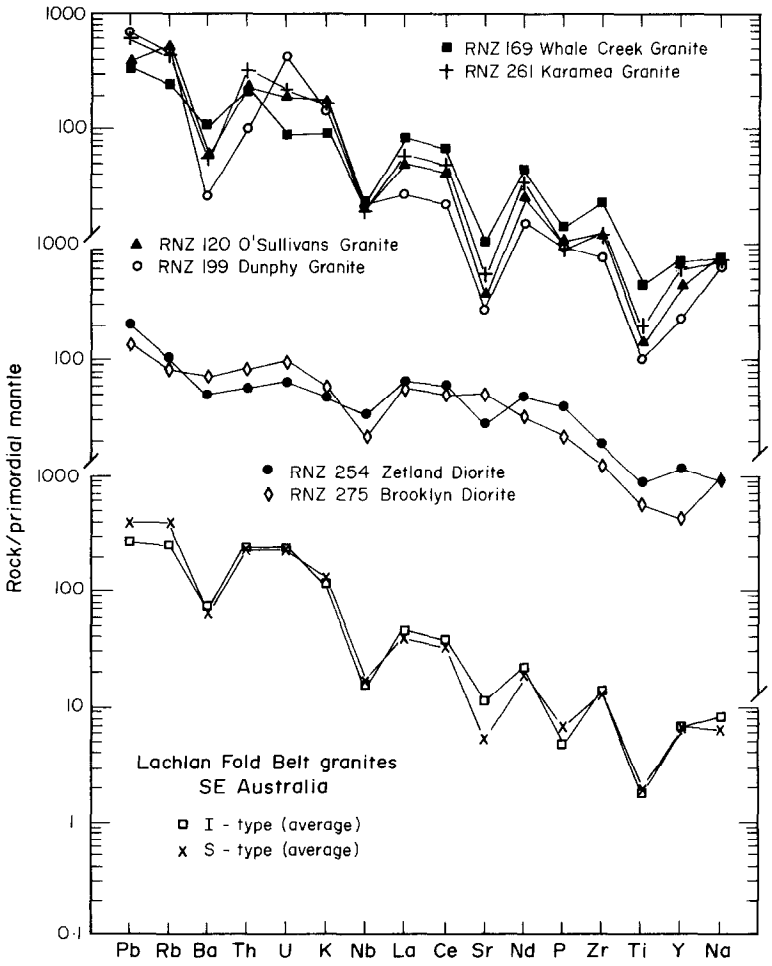

Fig. 7. Multi-element variation diagram illustrating the geochemical characteristics of the Karamea Batholith. Elements are arranged with increasing incompatibility, right to left, for spinel-lherzolite mantle assemblage. Nomalizing values after Sun and McDonough (1989).

Table 3
Sm–Nd whole-rock data for the Karamea Batholith and related rocks

	Sample	Sm (ppm)	Nd (ppm)	$^{147}Sm/^{144}Nd$	$^{143}Nd/^{144}Nd$	ϵ_{Nd} (375 Ma)	T_{DM} (Ga)
Whale Creek Granite	RNZ 169	11.37	62.50	0.1100	0.512212 ± 3	−4.1	1.22
	RNZ 173	10.10	54.97	0.1110	0.512232 ± 3	−3.8	1.20
O'Sullivans Granite	RNZ 120	7.50	39.00	0.1162	0.512160 ± 4	−5.4	1.38
	RNZ 271	7.86	44.02	0.1080	0.512293 ± 3	−2.4	1.08
Dunphy Granite	RNZ 194	5.77	22.65	0.1540	0.512059 ± 4	−9.2	2.53
	RNZ 199	5.89	28.63	0.1204	0.512089 ± 4	−7.2	1.62
	RNZ 212	5.53	27.20	0.1229	0.512088 ± 4	−7.2	1.60
	RNZ 222	8.78	42.83	0.1229	0.512088 ± 4	−0.7	1.60
Karamea Granite	RNZ 230	9.72	45.85	0.1282	0.512292 ± 3	−3.4	1.34
	RNZ 252	5.63	28.70	0.1186	0.512215 ± 4	−4.5	1.33
	RNZ 261	8.53	47.20	0.1092	0.512261 ± 3	−3.1	1.14
Barrytown Granite	RNZ BA	7.25	34.24	0.1280	0.512188 ± 4	−5.6	1.52
Zetland Diorite	RNZ 254	14.61	65.08	0.1357	0.512473 ± 4	−0.3	1.12
Riwaka Complex	RNZ 275	8.24	46.26	0.1077	0.512515 ± 3	+1.9	0.77

Grid references for samples are given in Table 2.

Granite showing the highest values (0.714–0.719). All ϵ_{Nd} values are negative and range from −0.3 in the Zetland Diorite to −9.2 in the Dunphy Granite. The Rameka Gabbro and the Brooklyn Diorite from the Riwaka Complex have primitive Sr and Nd isotopic compositions similar to the Zetland Diorite.

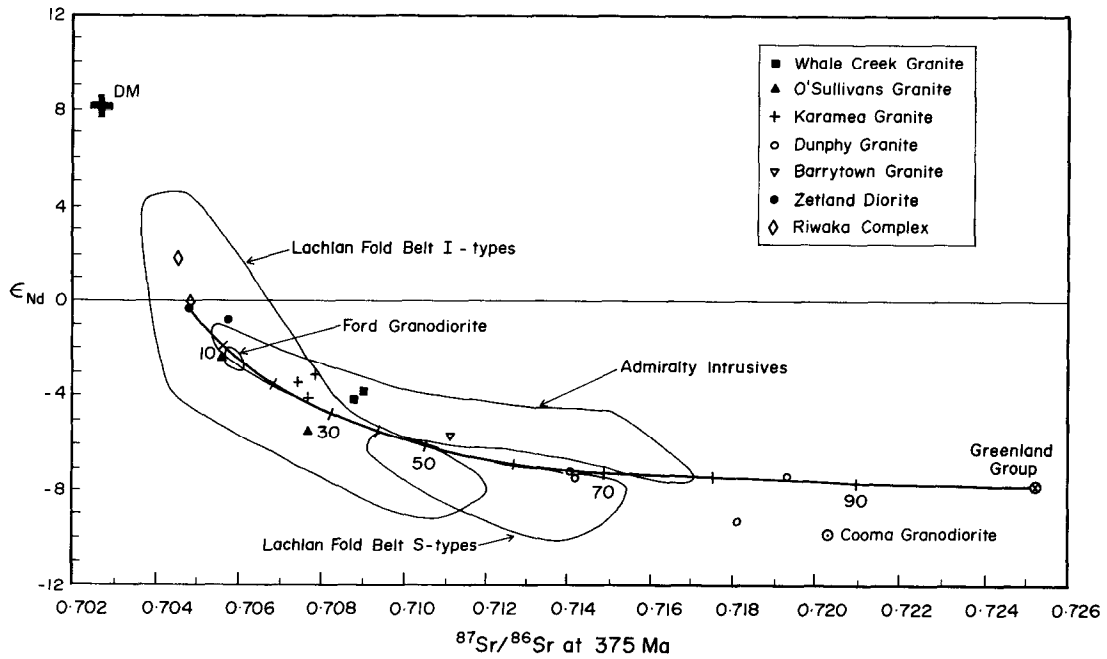

Fig. 8. ϵ_{Nd} (375 Ma) versus initial $^{87}Sr/^{86}Sr$ for the Karamea Batholith. Fields for I- and S-type granites from the Lachlan Fold Belt after McCulloch and Chappell (1982) and McCulloch and Woodhead (1993), Admiralty Intusives after Borg et al. (1987) and Ford Granodiorite after Weaver et al. (1992). Greenland Group data point is sample 33RO from Pickett and Wasserburg (1989) and the Cooma Granodiorite is from McCulloch and Chappell (1982).

In Fig. 8, all of these mafic samples plot close to Bulk Earth composition.

6. Granite types

The main criteria for distinguishing I- and S-type granites can be summarized as follows (see Chappell and White, 1992, for a comprehensive review): S-types are always peraluminous [alumina saturation index (ASI > 1.1)] and contain Al-rich minerals (e.g. Al-rich biotite, cordierite, muscovite, garnet, sillimanite, andalusite). Chemically, they are lower in Na, Ca, Sr and Fe^{3+}/Fe^{2+} and higher in Cr and Ni. I-types are metaluminous to weakly peraluminous (ASI < 1.1) and commonly contain biotite, hornblende and titanite. In terms of their isotopic compositions, S-type granites have higher $\delta^{18}O$ values (> 10‰) and more evolved Sr and Nd isotopic compositions (Fig. 8). I-type granites range in $^{87}Sr/^{86}Sr_{(i)}$ from 0.704 to 0.712 and in ϵ_{Nd} from +3.5 to −8.9. For the S-type granites, the corresponding values are 0.708 to 0.720 and −5.8 to −9.2. The S-type granites contain a diverse assemblage of metasedimentary enclaves, whereas enclaves in the I-types are commonly metaluminous and hornblende-bearing.

According to Tulloch (1983, 1988) and Cooper and Tulloch (1992), the mineralogy, chemistry and isotopic composition of the Karamea Batholith indicates that it is distinctly S-type in character. Certainly, the strongly peraluminous Dunphy Granite, which contains cordierite and has high Sr initial ratios and large negative ϵ_{Nd} values, fits the criteria for an S-type granite. However, the metaluminous, hornblende-bearing Zetland Diorite and the weakly peraluminous (ASI < 1.1) Whale Creek Granite have clear I-type characteristics. The Karamea Granite and the O'Sullivans Granite do not conform well to the I–S classification scheme. Their Sr and Nd isotopic compositions suggest an I-type designation, whereas their mineralogy (2-mica granites) and peraluminous compositions are characteristic of S-types. A similar compositional overlap has been observed in the Lachlan Fold Belt, where in the absence of associated mafic rocks, the more felsic and slightly peraluminous I-type granites are difficult to distinguish from the felsic S-type granites (Chappell and White, 1992). In summary, however, it is clear that in terms of the I–S classification, both types are represented in the Karamea Batholith. Moreover, there appears to be continuum in terms of chemical characteristics from one extreme to the other (e.g. Fig. 3).

7. Origin of the magmas

The strong inverse correlation between ϵ_{Nd} values and initial $^{87}Sr/^{86}Sr$ ratios for the Karamea Batholith (Fig. 8) suggests that the granites were generated by a simple two-component mixing process. In Fig. 8, the samples define a concave-upward curve between a mantle-like component and an evolved sedimentary crustal component. The mantle-like end-member is taken to be the Zetland Diorite/Riwaka Complex, and the crustal component is represented by the Ordovician Greenland Group. A mixing curve be-

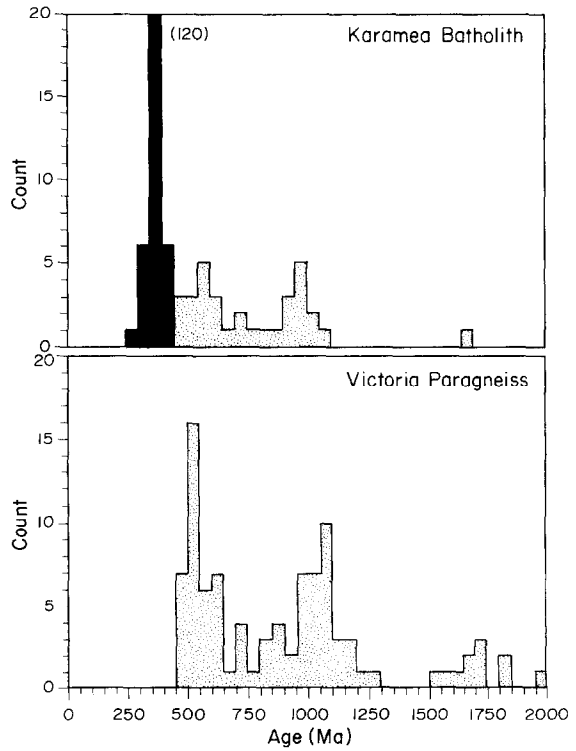

Fig. 9. Age distributions of zircons from the Karamea Batholith and related plutons and a sample of paragneiss, thought to be metamorphosed Greenland Group (Ireland, 1992; Muir et al., 1996).

tween these two components is shown in Fig. 8. The Whale Creek Granite, Karamea Granite and O'Sullivans Granite can be modelled by 20–30% crustal end-member, whereas the Dunphy Granite appears to represent 65–85% crustal material. The proportion of crustal material in the Dunphy Granite is similar to that estimated by Collins (in press) for the S-type granites in the Lachlan Fold Belt.

The large sedimentary component indicated by the isotopic data in the Dunphy Granite is supported by the presence of abundant metasedimentary enclaves, and by recent U–Pb zircon studies. SHRIMP analysis of the inherited zircon component in the Karamea Batholith has revealed distinct 500–600 Ma, 1000 Ma and a number of older components (Muir et al., 1994, 1996). The Dunphy Granite in particular contains a large amount of inherited zircon, with approximately two thirds of the crystals analysed giving ages significantly older than the magmatic age. The inherited zircon population in the Karamea Batholith is remarkably similar to the age pattern of detrital zircons from the Greenland Group (Fig. 9). Both contain major 500–600 Ma and 1000 Ma peaks, with a scatter of older ages. The close match of the inheritance pattern suggests that the older zircons in the granites were derived from the incorporation of Greenland Group rocks, rather than Proterozoic–Early Cambrian crystalline basement.

8. Comparisons with Australia and Antarctica

Before discussing the petrogenetic model for the Karamea Batholith in more detail, it is worth reviewing the models proposed for the Lachlan Fold Belt granites in SE Australia and coeval plutonic rocks in Antarctica.

8.1. Lachlan Fold Belt

The rocks forming the Karamea Batholith are similar to the I- and S-type granites of the Lachlan Fold Belt in terms of their age, petrography, major and trace element geochemistry, and Sr and Nd isotopic composition. On the basis of reliable U–Pb zircon and Rb–Sr data, the bulk of the Lachlan Fold Belt granites are slightly older than the the Karamea Batholith, and were emplaced between 440 and 380 Ma (I.S. Williams et al., 1992). However, both I- and S-type granites with younger ages down to ~ 360 Ma occur in the central part of the belt north of Melbourne (Richards and Singleton, 1981; Gray, 1990). In addition, Middle–Late Devonian granites are abundant in the Blue Tier Batholith in the northeastern part of Tasmania (Cocker, 1982; E. Williams et al., 1989).

Chappell and White (1992) argue that all granites in the Lachlan Fold Belt, whether S-type or I-type, were derived from melting of pre-existing continental crust. Direct input of mantle-derived material is not favoured, although a massive injection of conductive heat is postulated (Chappell, 1994).

The S-type Cooma Granodiorite in the Lachlan Fold Belt is thought to have formed by the ultrametamorphism of local Ordovician metasedimentary rocks (e.g. White and Chappell, 1988 and references therein). However, according to Chappell and White (1992), the chemical and isotopic compositions of most of the S-type granites suggest that they were not derived by direct melting of these metasedimentary rocks. Compared with the Ordovician greywackes, the S-type granites have higher concentrations of Na_2O and CaO, and lower $^{87}Sr/^{86}Sr$ initial ratios. Wyborn and Chappell (1983) and Chappell and White (1992) have therefore argued for the existence of a less mature and less isotopically evolved metasedimentary basement to the exposed Ordovician sediments.

The age pattern of inherited zircons in the Lachlan Fold Belt granites led I.S. Williams et al. (1992) to suggest that magmatism at 500–600 Ma and ~ 1000 Ma produced, through crustal underplating, the source for the I-type granites. At the same time, volcanism generated detritus that became the source for the S-type granites. The subsequent recycling of these rocks produced flysch that became incorporated into the Ordovician greywacke sequence.

The Sr and Nd isotopic data for the Australian granites (McCulloch and Chappell, 1982; McCulloch and Woodhead, 1993) form two overlapping fields, which together define a hyperbolic array in the lower right hand quadrant of the ϵ_{Nd} vs. $^{87}Sr/^{86}Sr_{(i)}$ diagram (Fig. 8). McCulloch and Chappell (1982) suggest that the isotopic array results from melting of a range of intracrustal source rocks having variable

ages and compositions. However, Gray (1984, 1990) has proposed that the array results from mixing between a basaltic end-member and a granitic melt (similar to Cooma Granodiorite) produced by melting of metasedimentary rocks.

Recently, Collins (in press) has demonstrated that the Moruya Suite in the Lachlan Fold Belt, which forms the most primitive end-member of the Sr–Nd mixing array [$^{87}Sr/^{86}Sr_{(i)} = 0.7041$ and $\epsilon_{Nd} = +3.0$], is itself a crust–mantle mix. Collins (in press) suggests that the granites are products of a 3-component mixing system of mantle-derived melts, Neoproterozoic–Cambrian arc-type lower crust and Ordovician metasedimentary material. The 3-component model requires that mantle-derived basaltic magmas intruded and underplated the lower crust, inducing melting. The resultant mixture, a low-K, low SiO_2 (~60%) tonalitic magma, represents the I-type parental material. The mantle component is represented by rare coeval gabbroic complexes associated with the granites. Under elevated geotherms, associated with the continued input of mantle-derived material, metasedimentary material in the middle crust was mobilised (= Cooma Granodiorite magma). The rising tonalitic I-type magmas then mixed with the Cooma-type magma to produce the S-type granites. Mixing calculations suggest that a typical S-type granite comprises ~70% Cooma-type magma and ~30% parental I-type magma. The distribution of the I-and S-type granites appears to be structurally controlled, with areas of abundant S-type granites corresponding to overthickened crust, where Ordovician metasedimentary rocks were underthrust to mid-crustal levels (i.e. into the melting zone).

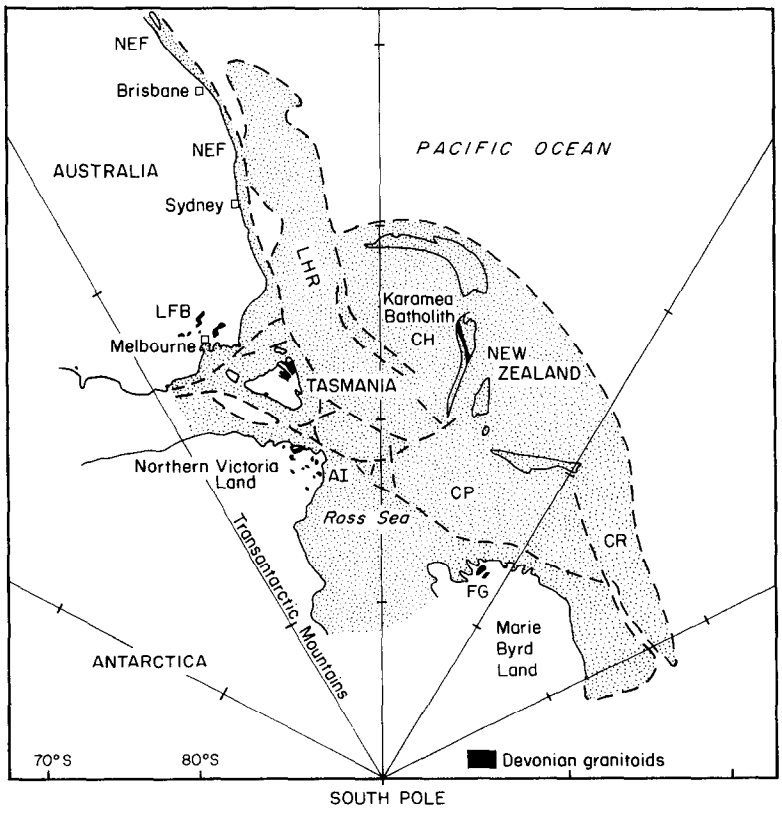

Fig. 10. Distribution of continental masses around the SW Pacific at 100 Ma (after Weaver et al., 1994). Stipple indicates thinned continental crust. *FG* = Ford Granodiorite, *AI* = Admiralty Intrusives, *LFB* = Lachlan Fold Belt, *NEF* = New England Fold Belt, *LHR* = Lord Howe Rise, *Ch* = Challenger Plateau, *CP* = Campbell Plateau, *CR* = Chatham Rise.

8.2. Antarctica

Plutonism of mid-Paleozoic age also occurred in the Bowers and Robertson Bay terranes in northern Victoria Land, and in Marie Byrd Land in western Antarctica (e.g., Adams, 1987; Borg et al., 1987; Weaver et al., 1991). In northern Victoria Land, the Admiralty Intrusives (Fig. 10) are a suite of calc-alkaline tonalites, granodiorites and monzogranites that give Rb–Sr whole-rock ages in the range 390–360 Ma. The rocks are predominantly metaluminous/I-type (ASI < 1.1), but according to Borg et al. (1987), there is a strong compositional polarity indicating increasing involvement of old crustal material from SW–NE. Initial $^{87}Sr/^{86}Sr$ ratios range from 0.705 to 0.717 and ϵ_{Nd} values at 375 Ma range from −0.8 to −7.1 (Borg et al., 1987). In Fig. 8, the isotopic data form a concave-upward array that lies above the field for the Lachlan Fold Belt S-types and the mixing line for the Karamea Batholith. However, samples of the Admiralty Intrusives with the least crust-like signature overlap with the field for the Lachlan Fold Belt I-types and the Whale Creek and Karamea Granites from New Zealand. Borg et al. (1987) have argued that the isotopic array for the Admiralty Intrusives indicates that the crustal source materials in Northern Victoria Land are different from those involved in the SE Australian granites. The Admiralty Intrusives were emplaced into Ordovician greywackes (Robertson Bay Group) that have been correlated with the Greenland Group in New Zealand (Bradshaw et al., 1985). However, there are no published isotopic data from the Robertson Bay Group that would enable further comparisons to be made.

In Marie Byrd Land, the Ford Granodiorite (Fig. 10) comprises biotite-rich, hornblende-bearing tonalites and granodiorites with Rb–Sr ages of 380–350 Ma (Adams, 1987; Weaver et al., 1991). The suite is calc-alkaline and metaluminous to weakly peraluminous (ASI < 1.1). Samples of the Ford Granodiorite have low initial $^{87}Sr/^{86}Sr$ ratios (0.704–0.706) and small negative ϵ_{Nd} values (ϵ_{Nd} at 375 Ma = −2 to −3) suggesting limited crustal input (< 10%). In Fig. 8, the data points form a tight cluster at the upper end of the mixing line for the Karamea Batholith. The Ford Granodiorite also intrudes Ordovician metasedimentary rocks (Swanson Formation) that have been correlated with the Greenland Group in New Zealand (Adams, 1986). The range of $^{87}Sr/^{86}Sr$ ratios for Swanson Formation at 375 Ma is 0.717–0.725 (recalculated from Adams, 1986; Adams et al., 1995), which encompasses the Greenland Group.

9. Discussion

The isotopic data and inherited zircon population in the Karamea Batholith point to simple mixing between a mantle-derived mafic magma with $\epsilon_{Nd} = 0$ and Paleozoic metasedimentary material. However, a mantle source with $\epsilon_{Nd} = 0$ is likely to be a large scale blend of depleted mantle material, that has $\epsilon_{Nd} = +4$ or higher, with lower crustal material (e.g. Rogers and Hawkesworth, 1989). Hence, a 3-component mixing model for the Karamea Batholith, similar to that proposed by Collins (in press) for the Lachlan Fold Belt in SE Australia, cannot be ruled out. It could be argued that the Zetland Diorite/Riwaka Complex is itself a mixture of mantle-derived basaltic magma (with $\epsilon_{Nd} \sim +4$ or higher) and Neoproterozoic–Cambrian arc-type crust. There is no field or isotopic evidence for such a primitive basaltic component in the Karamea Batholith, but there is certainly evidence for igneous activity in the Western Province around 500–600 Ma.

The oldest igneous rocks in New Zealand are the Middle Cambrian (~ 530 Ma) Heath Creek beds, Devil River Volcanics and the ultramafic Cobb Igneous Complex (Cooper, 1989) in the Takaka terrane (Fig. 1a) of NW Nelson. There are no published isotopic data from these rocks, but limited major and trace element data indicate a calc-alkaline/island-arc affinity (Cooper and Tulloch, 1992). Equivalents of the Cambrian rocks in the Takaka terrane also occur in Antarctica (Bradshaw et al., 1985) and in SE Australia (Crawford et al., 1984). The Cambrian Greenstone Belts in SE Australia contain boninites and tholeiites with ϵ_{Nd} values around +5 at 375 Ma (recalculated from Nelson et al., 1984). Again, however, there is no field evidence (e.g. mafic enclaves) or isotopic evidence for such a component in the Karamea Batholith.

At present, therefore, the components that mixed to produce the Zetland Diorite/Riwaka Complex magmas are unidentified, as is the time of mixing. Our model for generating the Karamea Batholith is closely similar to that proposed by Collins (in press) for the Lachlan Fold Belt granites. Mafic magmas, represented by the Zetland Diorite/Riwaka Complex, were produced from a mixed lithospheric mantle. These mafic magmas intruded the crust and encountered fertile Ordovician metasedimentary rocks at mid-crustal levels. The influx of this hot material initiated partial melting of the metasedimentary rocks, and the resultant anatectic melts mixed with the mafic magmas to produce hybrid granites.

10. Tectonic setting

The Karamea Batholith and the Riwaka Complex in New Zealand form part of an extensive Middle–Late Devonian belt of magmatic activity along, or close to, the Paleo-Pacific margin of Gondwana (Muir et al., 1994). In the continental reconstruction shown in Fig. 10, this belt can be traced for more than 2000 km from Australia through New Zealand and into Antarctica.

Little is known about the tectonic environment in New Zealand during the emplacement of the Karamea Batholith and the Riwaka Complex. Devonian sediments are rare and outcrops are confined to the Reefton area in the Buller terrane and the Baton River area in the Takaka terrane (Fig. 1). Both areas comprise shallow marine sedimentary rocks that were deposited close to a slowly subsiding continental margin (Cooper, 1989). There is no evidence for widespread orogenic activity at this time.

The tectonic setting of the Lachlan Fold Belt and the I- and S-type granites has been the subject of considerable debate. According to Chappell et al. (1988) the Australian granites do not have subduction-related geochemical signatures, although many workers have attempted to relate these rocks to subduction processes (e.g., Fergusson and Glen, 1992 and references therein). In the absence of a clear link between subduction and magmatism, alternative tectonic models have therefore been proposed. Wyborn (1992) and Collins (1994) have suggested that the granites were derived by partial melting of the lower crust in response to crustal thickening and lithospheric delamination. However, recently Zen (1995) has argued that the thermal requirements of magma genesis are more compatible with an extensional tectonic model. In contrast, the Antarctic granites are typically I-type, and have many of the geochemical characteristics of subduction-related magmas (Borg et al., 1987; Vetter and Tessensohn, 1987; Weaver et al., 1991).

Acknowledgements

RJM, SDW and JDB gratefully acknowledge the funding of the "New Zealand Granites and Crustal Evolution" programme by the Foundation for Research Science and Technology under contract UOC 313. The Department of Conservation are thanked for allowing access to the Tasman Wilderness Area in the new Kahurangi National Park. P.J. Forsyth, R. Fergusson and K.A. Watson are thanked for their assistance in the field. Isotope work was carried out at the NERC Isotope Geosciences Laboratory, Keyworth, with assistance from S. Noble and B. Barreiro. We are especially grateful to D. Shelley for helpful comments and for finding cordierite in the Dunphy Granite, and to W.J. Collins for providing a copy of his unpublished manuscript. C.M. Gray and P.J. Patchett are thanked for their constructive reviews.

References

Adams, C.J.D., 1986. Geochronological studies of the Swanson Formation of Marie Byrd Land, West Antarctica, and correlation with northern Victoria Land, East Antarctica and the South Island, New Zealand. N.Z.J. Geol. Geophys., 29: 345–358.

Adams, C.J.D., 1987. Geochronology of granite terranes in the Ford Ranges, Marie Byrd Land, West Antarctica. N.Z.J. Geol. Geophys., 30: 51–72.

Adams, C.J.D., Seward, D. and Weaver, S.D., 1995. Geochronology of Cretaceous granites and metasedimentary basement on Edward VII Peninsula, Marie Byrd Land, West Antarctica. Antarct. Sci., 7: 265–277.

Borg, S.G., Stump, E., Chappell, B.W., McCulloch, M.T., Wyborn, D., Armstrong, R.C. and Holloway, J.R., 1987. Granitoids of northern Victoria Land, Antarctica: Implications of chemical

and isotopic variations to regional crustal structure and tectonics. Am. J. Sci., 287: 127–165.

Bradshaw, J.D., Weaver, S.D. and Laird, M.G., 1985. Suspect Terranes and Cambrian Tectonics in Northern Victoria Land, Antarctica. In: D.G. Howell (Editor), Tectonostratigraphic Terranes of the Circum-Pacific Region. Circum-Pac. Counc. Energy Miner. Resour., Earth Sci. Ser., pp. 467–479.

Braithwaite, R.L. and Pirajno, F., 1993. Metallogenic Map of New Zealand. Inst. Geol. Nuclear Sci., Monogr., 3, 215 pp.

Brown, G.C., 1982. Calc-alkaline intrusive rocks: their diversity, evolution and relation to volcanic arcs. In: R.S. Thorpe (Editor), Andesites. Wiley, London, pp. 437–461.

Chappell, B.W., 1994. Lachlan and New England: Fold belts of contrasting magmatic and tectonic development. J. Proc. R. Soc. N.S.W., 127: 47–59.

Chappell, B.W. and White, A.J.R., 1974. Two contrasting granite types. Pac. Geol., 8: 173–174.

Chappell, B.W. and White, A.J.R., 1992. I- and S-type granites in the Lachlan Fold Belt. Trans. R. Soc. Edinburgh Earth Sci., 83: 1–26.

Chappell, B.W., White, A.J.R. and Hine, R., 1988. Granite provinces and basement terranes in the Lachlan Fold Belt, southeastern Australia. Aust. J. Earth Sci., 35: 505–521.

Cocker, J.D., 1982. Rb–Sr geochronology and Sr isotopic composition of Devonian granitoids, eastern Tasmania. J. Geol. Soc. Aust., 29: 139–158.

Collins, W.J., 1994. Upper- and middle-crustal response to delamination: and example from the Lachlan Fold Belt, eastern Australia. Geology, 22: 143–146.

Collins, W.J., in press. S- and I-type granitoids of the eastern Lachlan fold belt: 3-component mixing, not restite unmixing. Trans. R. Soc. Edinburgh Earth Sci.,

Cooper, R.A., 1989. Early Paleozoic terranes of New Zealand. J. R. Soc. N.Z., 19: 73–112.

Cooper, R.A. and Tulloch, A.J., 1992. Early Palaeozoic terranes in New Zealand and their relationship to the Lachlan Fold Belt. Tectonophysics, 214: 129–144.

Crawford, A.J., Cameron, W.E. and Keays, R.R., 1984. The association boninite, low-Ti andesite, tholeiite in the Heathcote Greenstone Belt, Victoria. Aust. J. Earth Sci., 31: 161–175.

DePaolo, D.J. and Wasserburg, G.J., 1976. Nd isotopic variations and petrogenic models. Geophys. Res. Lett., 3: 743–746.

Ewart, A., 1982. The mineralogy and petrology of Tertiary–Recent orogenic volcanic rocks: with special reference to the andesite-basaltic compositional range. In: R.S. Thorpe (Editor), Andesites. Wiley, London, pp. 25–95.

Fergusson, C.L. and Glen, R.A., 1992. The Palaeozoic Eastern Margin of Gondwanaland: Tectonics of the Lachlan Fold Belt, southeastern Australia and related orogens. Tectonophysics, 214, 461 pp.

Gill, K.R. and Johnston, M.R., 1970. The geology and nickel–copper sulphide mineralisation in the Graham Valley, northwest Nelson. N.Z. J. Geol. Geophys., 13: 477–494.

Gray, C.M., 1984. An isotopic mixing model for the origin of granitic rocks in southeastern Australia. Earth Planet. Sci. Lett., 70: 47–60.

Gray, C.M., 1990. A strontium isotopic traverse across the granitic rocks of southeastern Australia: Petrogenetic and tectonic implications. Aust. J. Earth Sci., 37: 331–349.

Gray, C.M., 1995. Discussion of Lachlan and New England: Fold Belts of contrasting magmatic and tectonic development by B.W. Chappell. J. Proc. R. Soc. N.S.W., 128: 29–32.

Grindley, G.W., 1961. Sheet 13, Golden Bay 1st ed., scale 1:250,000, Geological Map of New Zealand, Dep. Sci. Ind. Res., Wellington, New Zealand.

Grindley, G.W., 1971. Sheets S8, Takaka 1st ed., scale 1:63,360, Geological map of New Zealand, Dep. Sci. Ind. Res., Wellington, New Zealand.

Grindley, G.W., 1980. Sheet S13, Cobb 1st ed., scale 1:63,360, Geological Map of New Zealand, Dep. Sci. Ind. Res., Wellington, New Zealand.

Harrison, T.M. and McDougall, I., 1980. Investigations of an intrusive contact, northwest Nelson, New Zealand – 1. Thermal, chronological and isotopic constraints. Geochim. Cosmochim. Acta, 44: 1985–2003.

Ireland, T.R., 1992. Crustal evolution of New Zealand: Evidence from age distributions of detrital zircons in Western Province paragneisses and Torlesse Greywacke. Geochim. Cosmochim. Acta, 56: 911–920.

Kutsukake, T., 1988. The Britannia Granite pluton in the Karamea Batholith, South Island, New Zealand. N.Z. J. Geol. Geophys., 31: 275–286.

Landis, C.A. and Coombs, D.S., 1967. Metamorphic belts and orogenesis in southern New Zealand. Tectonophysics, 4: 501–518.

Mayes, C.L., Lawver, L.A. and Sandwell, D.T., 1990. Tectonic history and new isochron chart of the South Pacific. J. Geophys. Res., 95B: 8543–8567.

McCulloch, M.T. and Chappell, B.W., 1982. Nd isotopic characteristics of S- and I-type granites. Earth Planet. Sci. Lett., 58: 51–64.

McCulloch, M.T. and Gamble, J.A., 1991. Geochemical and geodynamical constraints on subduction zone magmatism. Earth Planet. Sci. Lett., 102: 358–374.

McCulloch, M.T. and Woodhead, J.D., 1993. Lead isotopic evidence for deep crustal-scale fluid transport during granite petrogenesis. Geochim. Cosmochim. Acta, 57: 659–674.

Mittlefehldt, D.W. and Miller, D.F., 1983. Geochemistry of the Sweetwater Wash Pluton, California: Implications for "anomalous" trace element behaviour during differentiation of felsic magmas. Geochim. Cosmochim. Acta, 47: 109–124.

Muir, R.J., Ireland, T.R., Weaver, S.D. and Bradshaw, J.D.,1994. Ion microprobe U–Pb zircon geochronology of granitic magmatism in the Western Province of the South Island, New Zealand. Chem. Geol., 113: 171–189.

Muir, R.J., Ireland, T.R., Weaver, S.D. and Bradshaw, J.D., 1996. Ion microprobe dating of Paleozoic granitoids: Devonian magmatism in New Zealand and correlations with Australia and Antarctica. Chem. Geol., 127: 191–210.

Nakamura, N., 1974. Determination of REE, Ba, Fe, Mg, Na and K in carbonaceous and ordinary meteorites. Geochim. Cosmochim. Acta, 38: 757–775.

Nathan, S., 1978. Sheets S31 and part S32, Buller–Lyell 1st ed.,

scale 1:63,360, Geological Map of New Zealand, Dep. Sci. Ind. Res., Wellington, New Zealand.

Nelson, D.R., Crawford, A.J. and McCulloch, M.T., 1984. Nd–Sr isotopic and geochemical systematics in Cambrian boninites and tholeiites from Victoria, Australia. Contrib. Mineral. Petrol., 88: 164–172.

Phillips, G.N., Wall, V.J. and Clemens, J.D., 1981. Petrology of the Strathbogie Batholith: a cordierite-bearing granite. Can. Mineralog., 19: 47–63.

Pickett, D.A. and Wasserburg, G.J., 1989. Neodymium and strontium isotopic characteristics of New Zealand granitoids and related rocks. Contrib. Mineral. Petrol., 103: 131–142.

Richard, P., Shimizu, N. and Allègre, C.J., 1976. $^{143}Nd/^{146}Nd$, a natural tracer: an application to oceanic basalts. Earth Planet. Sci. Lett., 31: 269–278.

Richards, J.R. and Singleton, O.P., 1981. Palaeozoic Victoria, Australia: igneous rocks, ages and their interpretation. J. Geol. Soc. Aust., 28: 395–421.

Roder, G.H. and Suggate, P.R., 1990. Sheet L29BD–Upper Buller Gorge, Geological Map of New Zealand 1:50,000. DSIR Wellington, New Zealand.

Rogers, G. and Hawkesworth, C.J., 1989. A geochemical traverse across the North Chilean Andes: evidence for crust generation from the mantle wedge. Earth Planet. Sci. Lett., 91: 271–285.

Sun, S.-S. and McDonough, W.F., 1989. Chemical and isotopic systematics of oceanic basalts: Implications for mantle composition and processes. In: A.D. Saunders and M.J. Norry (Editors), Magmatism in the Ocean Basins. Geol. Soc. London, Spec. Publ., 42: 313–345.

Tulloch, A.J., 1983. Granitoid rocks of New Zealand — a brief review. Geol. Soc. Am. Mem., 159: 5–20.

Tulloch, A.J., 1988. Batholiths, plutons and suites: nomenclature for granitoid rocks of Westland–Nelson, New Zealand. N.Z.J. Geol. Geophys., 31: 505–509.

Vetter, U. and Tessensohn, F., 1987. S- and I-type granitoids of north Victoria Land, Antarctica, and their inferred geotectonic setting. Geol. Rundsch., 76(1): 233–243.

Wall, V.J., Clemens, J.D. and Clarke, D.B., 1987. Models for granitoid evolution and source compositions. J. Geol., 95: 731–749.

Weaver, S.D., Bradshaw, J.D. and Adams, C.J., 1991. Granitoids of the Ford Ranges, Marie Byrd Land, Antarctica. In: M.R.A. Thomson, J.A. Crame and J.W. Thomson (Editors), Geological Evolution of Antarctica. Cambridge University Press, pp. 345–351.

Weaver, S.D., Adams, C.J., Pankhurst, R.J. and Gibson, I.L., 1992. Granites of Edward VII Peninsula, Marie Byrd land: anorogenic magmatism related to Antarctic–New Zealand rifting. Trans. R. Soc. Edinburgh Earth Sci., 83: 281–290.

Weaver, S.D., Storey, B.C., Pankhurst, R.J., Mukasa, S.B., Di-Venere, V.J. and Bradshaw, J.D., 1994. Antarctica–New Zealand rifting and Marie Byrd Land lithospheric magmatism linked to ridge subduction and mantle plume activity. Geology, 22: 811–814.

White, A.J.R. and Chappell, B.W., 1977. Ultrametamorphism and granitoid genesis. Tectonophysics, 43: 7–22.

White, A.J.R. and Chappell, B.W., 1983. Granitoid types and their distribution in the Lachlan Fold Belt, southeastern Australia. Geol. Soc. Am. Mem., 159: 21–24.

White, A.J.R. and Chappell, B.W., 1988. Some supracrustal (S-type) granites of the Lachlan Fold Belt. Trans. R. Soc. Edinburgh Earth Sci., 79: 169–182.

Williams, E., McClenaghan, M.P. and Collins, P.L.F., 1989. Mid-Palaeozoic Deformation, Granitoids and Ore Deposits. In: C.F. Burnett and E.L. Martin (Editors), Geology and Mineral Resources of Tasmania. Geol. Soc. Aust. Spec. Publ., 15: 238–292.

Williams, I.S., Chappell, B.W., Chen, Y.D. and Crook, K.A.W., 1992. Inherited and detrital zircons — vital clues to the granite protoliths and early igneous history of southeast Australia. Trans. R. Soc. Edinburgh Earth Sci., 83: 503.

Wyborn, D., 1992. The tectonic significance of Ordovician magmatism in the eastern Lachlan Fold Belt. Tectonophysics, 214: 177–192.

Wyborn, L.A.I. and Chappell, B.W., 1983. Geochemistry of the Ordovician and Silurian greywackes of the Snowy Mountains, southeastern Australia: an example of chemical evolution of sediments with time. Chem. Geol., 39: 81–92.

Zen, E-an., 1986. Aluminium enrichment in silicate melts by fractional crystallisation: some mineralogic and petrographic constraints. J. Petrol., 27: 1095–1118.

Zen, E-an., 1995. Crustal magma generation and low-pressure high-temperature regional metamorphism in an extensional environment: possible application to the Lachlan Fold Belt, Australia. Am. J. Sci., 295: 851–874.